Physical and Numerical Model of Electrocoagulation Process with Aluminum Electrodes for Phosphate Removal

Halkijević, Ivan; Lončar, Goran; Posavčić, Hana; Vouk, Dražen

Environment Protection Engineering

Vol. 48 2022 No. 3

DOI: 10.37190/epe220305

IVAN HALKIJEVIC (ORCID: 0000-0003-0694-3993)[1]
GORAN LONCAR (ORCID: 0000-0002-6466-3677)[1]
HANA POSAVCIC (ORCID: 0000-0001-6555-482X)[1]
DRAZEN VOUK (ORCID: 0000-0002-1458-7768)[1]

PHYSICAL AND NUMERICAL MODEL OF ELECTROCOAGULATION PROCESS WITH ALUMINUM ELECTRODES FOR PHOSPHATE REMOVAL

The efficiency of the electrocoagulation process for the removal of phosphate ions (PO_4^{3-}-P) has been analyzed using a batch full-scale reactor with aluminum electrodes. The effects of the flow rate through the reactor applied current density, and reactor volume were the focus of the study. The initial (PO_4^{3-}-P) concentration was reduced by 90% after 90 min of reactor operation time. Additionally, a three-dimensional numerical model for PO_4^{3-}-P removal via the electrocoagulation process is developed that includes the processes of phosphate adsorption and desorption on coagulated/flocculated particles, along with particles settling. Numerical model parametrization relies on the results from the experiments.

1. INTRODUCTION

The presence of phosphorus in wastewaters is to a large extent a consequence of human activities such as industry, agriculture, and livestock farming. The usual range of phosphorus concentrations in wastewater from households and industry is 3–15 mg/dm^3 [1], whereby the usual condition of maximum permissible concentrations of total phosphorus in effluent water from the purification facilities is 1.0 mg P_{tot}/dm^3 [2]. The total phosphorus limit values are defined by the EU guidelines and depend on the size of the wastewater treatment plant (2.0 mg P_{tot}/dm^3 for <10 000 PE and 1.0 mg P_{tot}/dm^3 for >100 000 PE). Usually, phosphorus in a solution can be in the form of orthophosphates,

[1]University of Zagreb, Faculty of Civil Engineering, Fra Andrije Kacica-Miosica 26, 10 000 Zagreb, Croatia, corresponding author I. Halkijevic, email address: ivan.halkijevic@grad.unizg.hr

polyphosphates, and organic phosphates. Common forms of phosphate ions in the solution include orthophosphates, polyphosphates, and organic phosphates, [3]. The principal component of phosphorus in wastewaters is orthophosphate with a less concentrated organic phosphorus compound [4]. Common phosphorous removal techniques are chemical adsorption and precipitation [5, 6], ion exchange, electrodialysis, membrane filtration, and electrocoagulation.

The removal of phosphate from water is based on the conversion of the dissolved phosphates to an insoluble solid phase. Generated insoluble phase can be subsequently removed by sedimentation or flotation. The most common wastewater treatment techniques rely on phosphate precipitation in the presence of dissolved Al^{3+}, Ca^{2+}, and Fe^{3+} cations, and to a lesser extent Fe^{2+}. It is known that iron and aluminum are present in water in form of $FePO_4$ and $AlPO_4$ at pH < 6.5, while at pH > 6.5 iron and aluminum are strongly converted to oxides [6].

Due to the increased standards and legislative regulations set on effluent water quality, electrochemical technologies increasingly attract attention in the field of wastewater treatment [7]. It is suggested that this method potentially can replace some of the conventional water treatments [8].

Electrocoagulation (EC) is a process of metal hydroxide flocs generation due to electrodissolution of a soluble anode, commonly made of aluminum (Al) or iron (Fe) [7–9]. The difference between electrocoagulation and chemical coagulation is the way of generating aluminum ions. The EC process requires no chemical additives. The coagulants are produced in situ, within the reactor by the electrolytic oxidation of the appropriate anode materials. The success of the electrocoagulation process is manifested through the action of the current on the colloids, suspensions, and emulsions by neutralizing the surface charge, and consequently combining several particles into the larger agglomerates [7, 8, 10]. Al electrodes have a higher degree of effluent removal efficiency and consume less energy than Fe electrodes [9]. After the processing with Al electrodes, the effluent is very clean and stable, while Fe electrodes initially give greenish color, followed by yellow color. Green and yellow colors indicate the generated Fe^{2+} and Fe^{3+} ions [10]. The precipitated flocs layer produced by EC phosphate removal without additional electrolytes (such as NaCl) is usually a mixture of $Al(OH)_3$ and $AlPO_4$ [11].

Irdemez et al. [6, 9] studied the influence of pH and initial phosphate concentration on the electrochemical treatment process with Al and Fe electrodes. They concluded that pH is the key parameter and that the highest removal efficiency is achieved with Al electrodes at pH = 3. The influence of sodium chloride (NaCl) concentration as an electrolyte was analyzed by Chen et al. [10] and Kabdasli et al. [12], and it was concluded that, except for the positive effect of Al^{3+} increase, due to the increase of solution conductivity, there was also a secondary positive effect shown in disabling the formation of the passivation layer on the Al electrode surface. Relevant published studies involved only small-scale laboratory reactors, so the main objective of this study is to

investigate the effectiveness of EC in a full-scale reactor with Al electrodes for the removal of phosphate. The other objective is to create a mathematical model for the whole process so that some hydraulic effects of the constructive (design) elements of the reactor can be further investigated.

2. BASICS OF EC THEORY

The electrocoagulation process is conducted through three successive phases. In the first phase, the coagulant is formed through electrolytic oxidation of sacrificial electrode, i.e., anode. The activity of direct current on electrodes in the electrochemical cell results in anode oxidation and cathode reduction. The cathode generates hydrogen with the consequence of increasing the pH of the solution

$$2H^+ + 2e^- \rightarrow H_2 \tag{1}$$

$$2H_2O + 2e^- \rightarrow H_2 + OH^- \tag{2}$$

For Al anode, the chemical reaction for the production of $Al(OH)_3$ is defined as

$$Al \rightarrow Al^{3+} + 3e^- \tag{3}$$

$$Al^{3+} + 3OH^- \rightarrow Al(OH)_3 \tag{4}$$

The oxygen generation on the anode

$$2H_2O \rightarrow O_2 + 4H^+ + 4e^- \tag{5}$$

Faraday's law of electrolysis allows a theoretical estimate of dissolved ions Al^{3+} amount due to the anode operation. The law defines the ratio of the electric current I and the electrolyte-generated mass m within the electrochemical cell

$$m = \phi \frac{It}{zF} M \tag{6}$$

where: m is the mass of dissolved electrode material in, g, t is the electrode working time, h, I is applied current, A, M is the molar mass of the electrode material in g/mol, z is the number of electrons in oxidation/reduction reaction (3 for Al^{3+}), F is the Faraday constant (96 485.3 C/mol) and ϕ is the correction coefficient of electrolyte dissociation efficiency. It is noted that the efficiency of dissociation may be greater than the one specified by Faraday's law [7, 8].

Al^{3+} ions (eqs. (3) and (4)) are currently subjected to a further spontaneous reaction to the production of the corresponding hydroxide (eq. (4)). Except hydroxides, Al^{3+} ions also form monomers and polymers, depending on the pH range [13]. After that, the

destabilization of contaminants and particulate suspensions, and their aggregation to the formation of flocs, occur [14]. The mechanism, i.e., the detailed flocculation model is shown in [15]. In the electrocoagulation process, coagulation and flocculation occur simultaneously, as opposed to chemical coagulation.

3. MATERIALS AND METHODS

A full-scale EC reactor was constructed in the hydrotechnical laboratory at the Faculty of Civil Engineering, University of Zagreb. The reactor has two rectangular tanks, whose dimensions are 0.80 × 0.55 × 1.10 m. The first tank is used for EC process from which water is pumped between two rectangular electrodes in separate casings outside the tank. The total surface of Al electrodes is 0.063 m^2 (2 × 0.98 × 0.032 m) with an electrode distance of 0.5 cm. A secondary tank is used for settling. The photograph and the process scheme of the reactor are shown in Fig. 1, while the schematic view with the corresponding measurement positions is shown in Fig. 2.

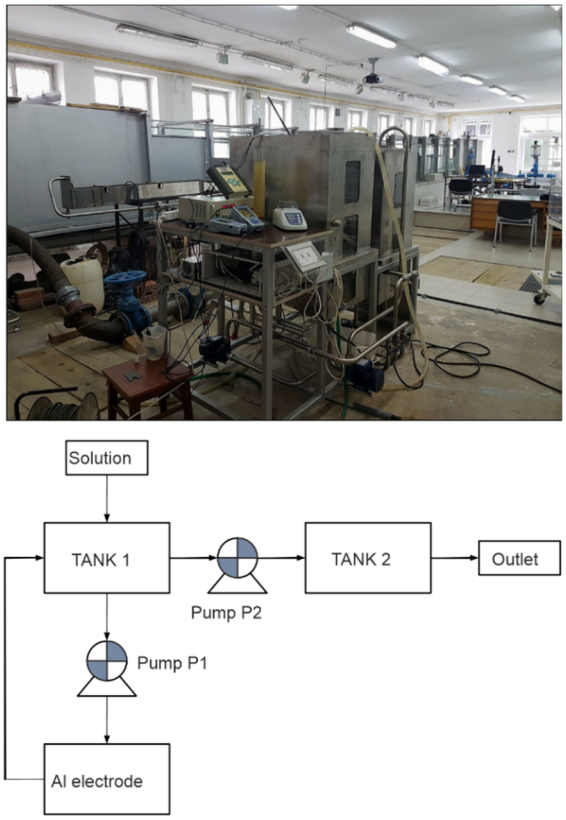

Fig. 1. Photograph (upper) and the process scheme (lower) of the EC reactor

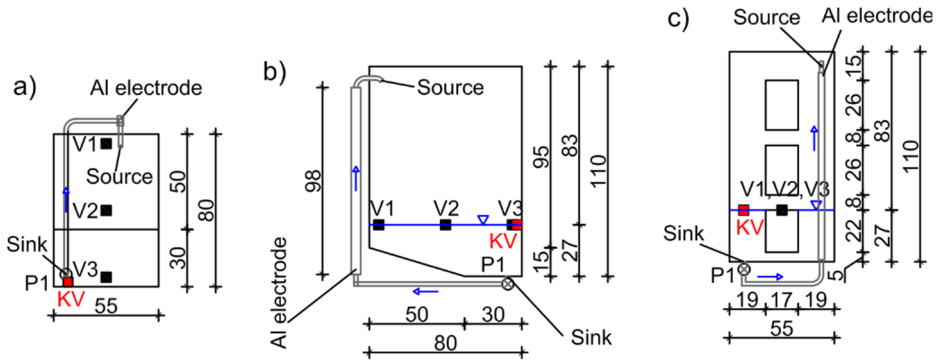

Fig. 2. Schematic representation of the EC reactor indicating the velocity measurement positions (V1–V3) at a depth of 5 cm and the water sampling position for the measuring water-quality parameters of the surface layer (KV): a) top view, b) side view, c) front view

The whole water-treatment process is divided into several phases. Initially, the first tank is filled with drinking water from the public water supply system to a depth h of 0.275 m or 0.5 m (90 dm^3 or 180 dm^3, Fig. 2). After adding 0.23 cm^3 of 85% H_3PO_4 solution and stirring until a homogeneous initial PO_4^{3-}-P concentration of 3.8 mg/dm^3 is reached, an appropriate amount of NaCl is added to achieve homogeneous initial concentrations of 2 g/dm^3. Subsequently, pump P1 (Fig. 1) is activated to transport water from the bottom of the tank through the Al electrodes casing with a specific flow rate of 0.05 or 0.15 dm^3/s. The flow rate is regulated with a variable frequency drive installed on pump P1. The water returns to the tank in the form of a free-falling jet, impinging the water surface approximately below the position of the source, Fig. 2. The total reaction time is 90 min. After 90 min, the water is pumped to the secondary tank for settling by using pump P2.

Water samples for measurements are taken at the KV position (Fig. 2), prior to the activation of the electrodes (initial state) and after every 30 min. Measurements were taken for phosphate concentrations (PO_4^{3-}-P), dissolved oxygen (DO) and Al (Al^{3+}) concentrations, as well as for the water temperature and pH. The velocity was measured at three points, V1, V2 and V3 (locations shown in Fig. 2), at a depth of 5 cm. Velocity recording period was set to 1 min for each measurement point.

For the PO_4^{3-}-P and Al^{3+} concentrations, a digital photometer (NANOCOLOR 500D, Eutech) with a photometric accuracy of ±1% was used. Method 0762 (Test 0-76, Ref. 985 076) and method 0981 (Test 0-98, Ref. 985 098) were applied for the PO_4^{3-}-P and Al^{3+} measurements, respectively. The flow was measured using an ultrasonic meter (FLUXUS F601, Flexim). The water temperature, pH (resolution 0.001, accuracy ±0.002) and DO concentration (resolution 0.01 mg/dm^3, accuracy ±0.2 mg/dm^3) were measured using a Multiprobe CyberScan PCD 650 (Eutech). The velocities were measured using a 3D

acoustic meter (Vectrino, Nortek, the diameter of the sampling volume 6 mm, accuracy ±0.5%).

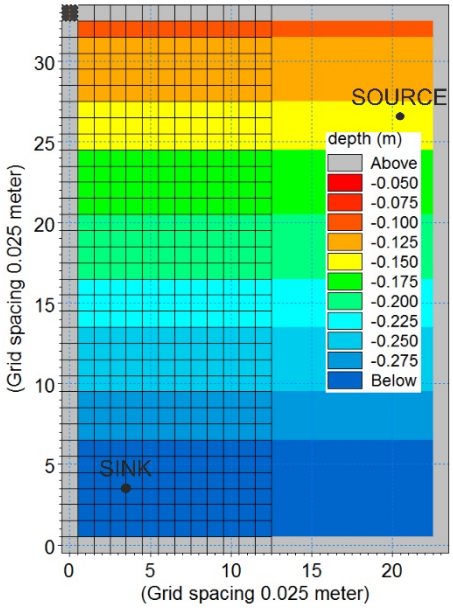

Fig. 3. Spatial discretization of the model domain (structured calculation mesh)

Numerical simulations were performed using a 3D numerical model Mike 3 (by DHI). The geometry of the reactor, including the sink (intake) and source positions, is similar to the physical and numerical models. For the numerical model, the intake (sink) position of the pipe connecting the tank with the Al electrodes and the pipe outlet (source) position in the tank are defined according to the physical model (EC reactor) and remain unaltered during the study. The model is based on the finite differential method, with the z coordinate system in the vertical direction and structured spatial discretization. Horizontally, the spatial domain (Fig. 3) is discretized by an equidistant step: $\Delta x = \Delta y = \Delta z = 0.025$ m (22 × 32 × 11 cells). The mathematical foundation of Mike 3 comprises the mass-conservation equation; the Reynolds-averaged Navier –Stokes equations, including the effect of the turbulence and variable density and the conservation equations for scalar fields. The model employs the artificial compressibility method [16–18] and the alternating direction implicit technique to integrate the equations for mass and momentum conservation in the space-time domain[19]. The equation matrices were resolved by a double-sweep algorithm and discretized on an Arakawa C-grid with second-order accuracy [20]. The 3D Quickest-Sharp scheme was used for the analysis of the transported scalar fields [21, 22]. The turbulent closure model used within Mike 3 relies on a k-ε formulation in the vertical direction [16, 23] and the Smagorinsky concept in the horizontal direction [24].

The EC process, thus the transport model, was implemented via an appropriate mathematical formulation that interprets the concentration change of dissolved and suspended substances through the interaction links with certain variables in the EC process.

4. MODELING AND MEASUREMENT RESULTS

The model of the PO_4^{3-}-P concentration change for water treatment via the EC process with Al electrodes includes the creation and settling of flocs, as well as the processes of PO_4^{3-}-P adsorption and desorption on the flocs. The numerical simulations show changes in the PO_4^{3-}-P concentration fields of the dissolved and suspended fractions through the water column. It is assumed that the organic fraction is negligible and that the PO_4^{3-}-P concentration in water is divided into two fractions: dissolved (PO_4^{3-}-P_D) and adsorbed onto flocculated particles ((PO_4^{3-}-P_A). Therefore, three process variables are defined: the concentration (PO_4^{3-}-P_D) and (PO_4^{3-}-P_A) fractions in the water column and the concentration of suspended particles (flocs) in the column of water, γ_S. For each process variable, corresponding differential equations describing the rate of change are proposed:

- The equation for the PO_4^{3-}-P_D concentration in the water column is as follows

$$\frac{d\left(PO_4^{3-}\text{-}P_D\right)}{dt} = K_A\left(PO_4^{3-}\text{-}P_D\right) \tag{7}$$

$$K_A = \frac{k_a}{\gamma_S} \tag{8}$$

where, k_a is the coefficient of adsorption on flocs, K_A is the adsorptive velocity coefficient.

- Equation (9) defines the concentration dynamic of PO_4^{3-}-P_A adsorbed on flocs, while eq. (10) describes the sedimentation process participation

$$\frac{d\left(PO_4^{3-}\text{-}P_A\right)}{dt} = K_A\left(PO_4^{3-}\text{-}P_D\right)\gamma_S - \text{sed}\left(PO_4^{3-}\text{-}P_A\right) \tag{9}$$

$$\text{sed}\left(PO_4^{3-}\text{-}P_A\right) = w_S\frac{PO_4^{3-}\text{-}P_A}{dz} \tag{10}$$

where, w_S is the floc settling velocity, and dz is the cell thickness (height).

• The change in the mass concentration of flocs in time $d\gamma_S/dt$ is expressed by the following equation, which also contains sedimentation part sed(γ_S)

$$\frac{d\gamma_S}{dt} = -\text{sed}(\gamma_S) + S\gamma_S \tag{11}$$

$$\text{sed}(\gamma_S) = w_S \frac{\gamma_S}{dz} \tag{12}$$

Here, $S\gamma_S$ is the local source/sink of suspended particles (flocs) in the water column.

To adopt a rational value for $S\gamma_S$ (eq. (11)) in the numerical simulations, several steps are performed. First, the amount of metal generated (dissolved) due to anodic oxidation is calculated according to Faraday's law (eq. (6)). Here, the adopted values are t = 1.5 h, I = 3 A or 5 A, M = 27 g/mol, z = 3, F = 96 487 C/mol, ϕ = 1. Accordingly, the intensity of the source is adopted with the value $S\gamma_S$ = 9.4 mg/(dm^3·s) for the reactor flow rate of 0.05 dm^3/sand, I = 5 A).

The exponential formulation proposed in [25] (eq. (13)) is used for w_S, and slightly modified as indicated by eqs. (10) and (12).

$$w_S = \frac{k_w(1-n_1\gamma_S)^4}{\gamma_S}\frac{\exp(-n_2\gamma_S)}{\gamma_S} \tag{13}$$

where, k_w, n_1 and n_2 are the parameters (constants) of the floc settling-velocity model.

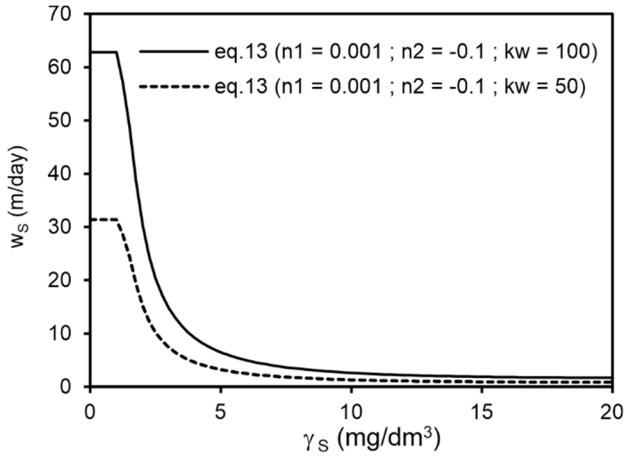

Fig. 4. Settling velocity depending on the mass concentration of the flocs γ_S and coefficient k_w according to the eq. (13)

The settling velocities depending on the mass concentration of the flocs γ_S are shown in Fig. 4. It can be noticed that the formulation of settling velocity according to

eq. (13), results in a continuous reduction of settling velocity upon increasing concentration. To determine the optimal values of the model constants K_A, k_W, n_1 and n_2 (model parameterization), the results from the measurement of the EC reactor were used. Measurements have shown that the optimal values for n_1 and n_2 ($n_1 = 0.001$, $n_2 = -0.1$) are the same for all experiments, while the best matching value of the k_W coefficient for Al electrodes was 100 for $K_A = 10^7$ dm^3/(mg·day).

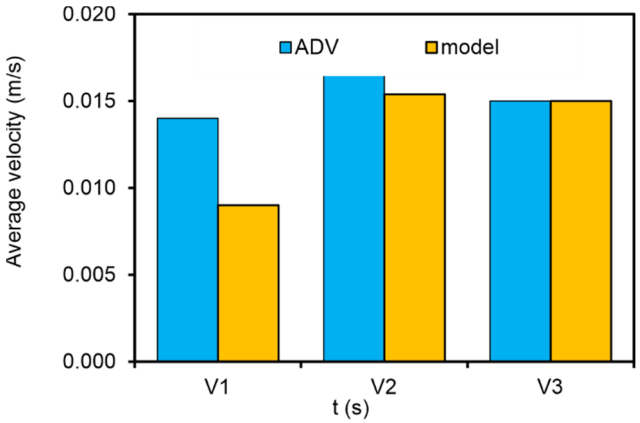

Fig. 5. Average measured and modeled flow velocities and corresponding standard deviations for three flow-velocity measurement positions (1 min averaging period)

Figure 5 shows the average measured and modeled flow velocities for three measurement positions during the operation of the Al reactor with a flow rate of 0.15 dm^3/s. The average measured flow velocities, although very small, are higher than the modeled ones. Their general layout, regarding the measurement positions, is similar.

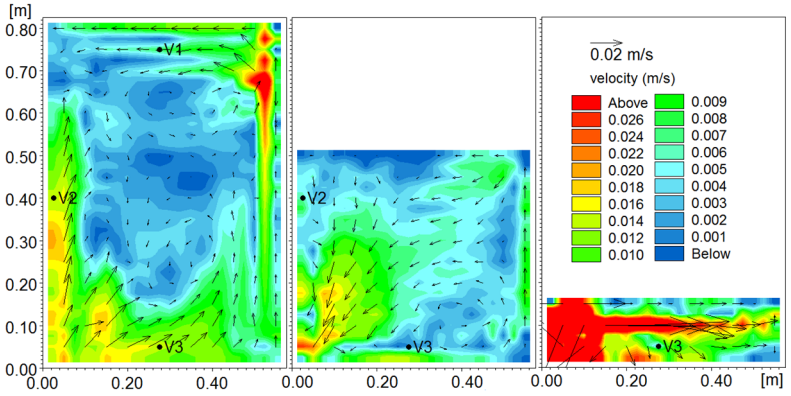

Fig. 6. Model horizontal velocity field for the surface (–1 cm, left), intermediate (–13 cm, middle), and bottom (–27 cm, right) layers during the operation of the Al reactor with a flow rate 0.15 dm^3/s (chamber filled with 90 dm^3)

Figure 6 shows the modeled horizontal velocity field for the surface, intermediate, and bottom layers (1, 13 and 27 cm below the water surface) during the operation of the Al reactor with a flow rate of 0.15 dm^3/s (experiment 3 and 4). The velocity increases near the source and sink, as expected.

Five experiments were performed using the reactor (Table 1). The measured values of the monitored water-quality parameters were used for obtaining appropriate values of the constants in the kinetic model (parameterization of numerical transport model).

Table 1

Description of experiments of the physical model

Experiment	Q [dm^3/s]	V_1 [m^3]	I [A]	i [A/m^2]	Decrease PO_4^{3-}-P_0 [%] (PO_4^{3-}-P_0 → PO_4^{3-}-P_{90}; ΔPO_4^{3-}-P_{90} [mg/dm^3]]
1	0.05	0.09	5	75	88 (3.8 →0.5; 3.3)
2	0.05	0.09	3	45	68 (3.8 →1.2; 2.6)
3	0.15	0.09	5	75	90 (3.8 →0.4; 3.4)
4	0.15	0.09	3	45	64 (3.8 →1.4; 2.4)
5	0.05	0.18	5	75	62 (3.8 →1.5; 2.3)

Initial concentration PO_4^{3-}-P_0 is 3.8 mg/dm^3, concentration PO_4^{3-}-P_{90} and decrease ΔPO_4^{3-}-P_{90} after 90 min of Al reactor activity; Q – flow through reactor, i – current density, V_1 – water volume within the tank.

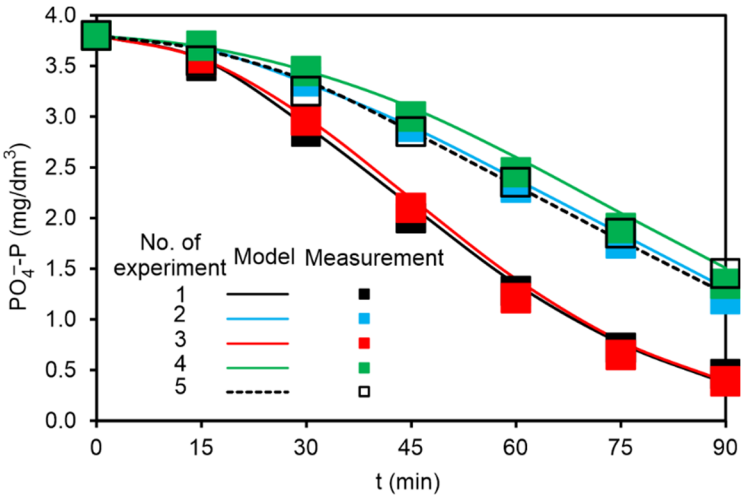

Fig. 7. Measured and modeled time series of PO_4^--P concentrations at the position KV (X = 8 cm, Y = 0 cm, Z = –3.5 cm/–24 cm below water surface) for experiments 1–5

Figure 7 shows the measured and the modeled time series of the PO_4^{3-}-P concentrations at the measurement position KV (X = 8 cm, Y = 0 cm, Z = –3.5 cm or –24 cm: 3.5 cm below the water surface in the case of a chamber filled with 90 dm^3, 24 cm in the case of a chamber filled with 180 dm^3) for experiments 1–5 (Table 1). The results of the numerical simulations (Fig. 7) were obtained by adopting the following values of the constants and transport-model parameters: $K_A = 3.25\times10^6$ dm^3/(mg·day), $k_W = 60$, $n_1 = 0.001$ and $n_2 = -0.1$. Figure 7 shows that the highest efficiency of removal is achieved by using the current density of 75 A/m^2 (experiments 1 and 3, Table 1). The removal efficiency in this study is almost independent of the flow rate through Al electrode reactor.

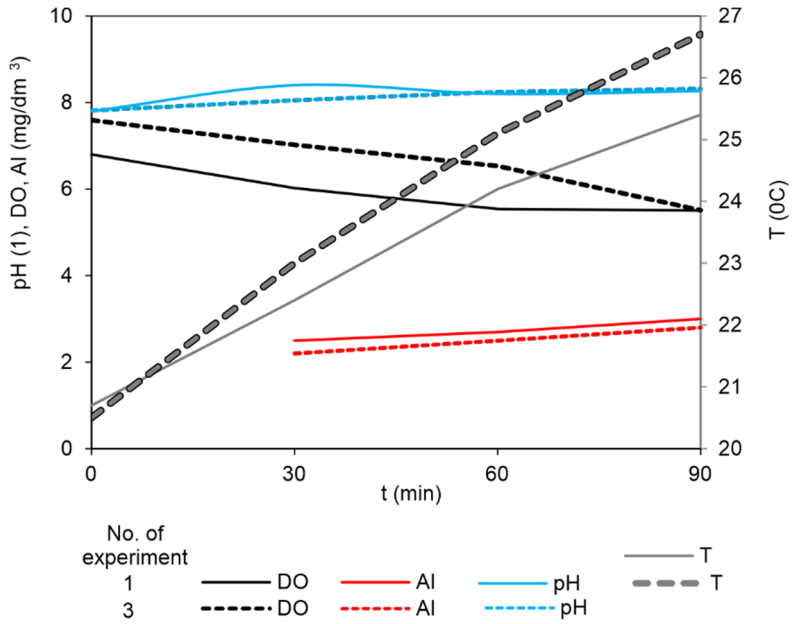

Fig. 8. Measured values of Al^{3+} and DO concentrations, as well as the water temperature and pH at the position KV (X = 8 cm, Y = 0 cm, Z = –3.5 cm, 3.5 cm/–24 cm) in experiments 1 and 3

Figure 8 shows the measured concentrations of Al^{3+} and DO, along with the pH and water temperature, at the position KV in experiments 1 and 3 (Table 1). The values are obtained in the initial state (0 min) and after every 15 min.

Figure 9 shows the modeled horizontal PO_4^{3-}-P_D concentration fields after 90 min of Al electrode operation with flow rates of 0.05 and 0.15 dm^3/s. It indicates approximately homogeneous PO_4^{3-}-P_D concentrations in the horizontal and vertical directions under the conditions of experiment 3 (Q = 0.15 dm^3/s). The calculated PO_4^{3-}-P_D field under the conditions of experiment 1 (Q = 0.05 dm^3/s) exhibits stronger pronounced

variation, primarily because of the weaker water mixing. Under the conditions of experiment 1 (Q = 0.05 dm^3/s), the PO_4^{3-}-P_D concentration in the surface layer varies from 0.35 mg/dm^3 to the maximum value of 0.4 mg/dm^3, and that in the bottom layer varies from 0.36 to 0.39 mg/dm^3. On the other hand, under the conditions of experiment 3 (Q = 0.15 dm^3/s), the concentration of PO_4^{3-}-P_D varies within a narrower range, between the minimum value of 0.384 mg/dm^3 and the maximum value of 0.390 mg/dm^3.

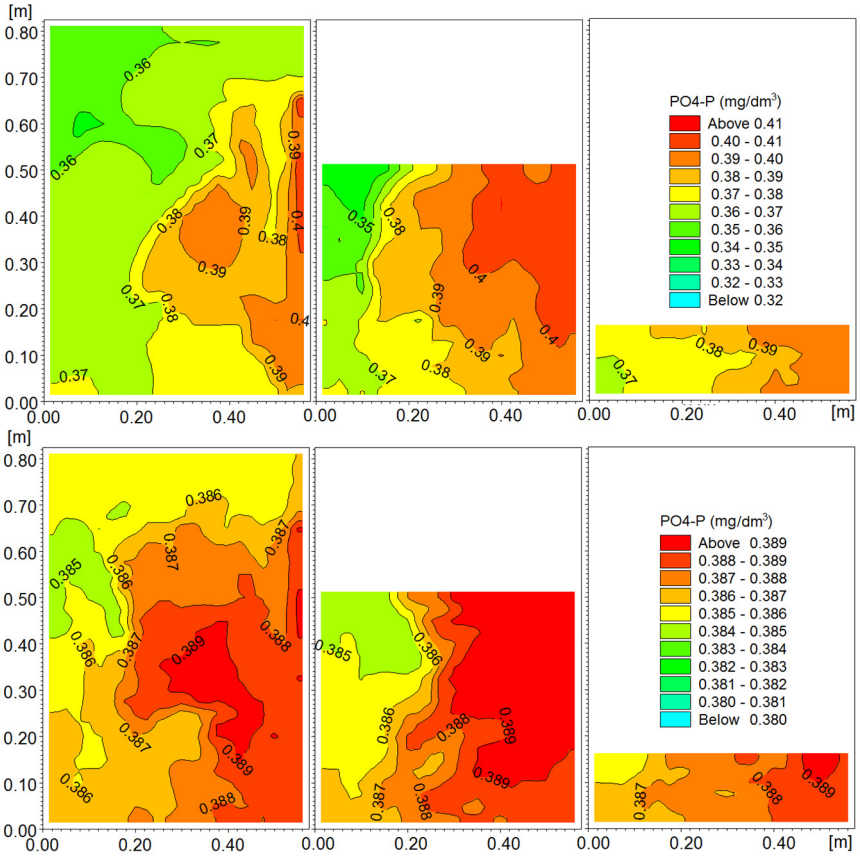

Fig. 9. Modeled horizontal PO_4^{3-}-P_D D concentration fields in the surface (–1 cm, left), intermediate (–13 cm, middle), and bottom (–27 cm, right) layers after 90 min of Al electrode operation (upper, the flow rate of 0.05 dm^3/s; lower, 0.15 dm^3/s; 90 dm^3 in a chamber)

5. ESTIMATION OF OPERATIONAL COSTS FOR EC REACTOR

The estimation of the operational costs (OC) of the EC reactor is given regarding the energy costs (electricity used by electrodes and pumps) and material (electrode) costs

$$OC = a\left(C_{\text{el}} + C_{\text{pump}}\right) + bC_{\text{mat}} \tag{14}$$

where: C_{el} is the electric energy consumption of 1 m^3 of treated water, kWh/m^3, C_{pump} is the electric energy consumption of the pump for 1 m^3 of treated water, kWh/m^3, and C_{mat}, kg Al/m^3, is the cost of the electrode material used in 1 m^3 of the treated water; a is the average electricity price (0.13 €/kWh according to the national tariff models), and b is the average market price of aluminum given as 1.54 €/kg. The electricity consumption C_{el}, kWh/m^3, is calculated according to the following expression

$$C_{\text{el}} = \frac{UIt}{V} \tag{15}$$

where U is the power supply voltage, V, I is the power supply current, A, t – the duration of the electrocoagulation process, h, V is the effective volume of the treated water, m^3.

The electricity consumption of the pump, kWh/m^3, is calculated according to the following expression

$$C_{\text{pump}} = \frac{Pt}{V} \tag{16}$$

where P is the nominal pump power, kW. In this study, electricity consumption is roughly estimated for a Pedrollo PKm 65 pump with a nominal output power of 0.55 kW [26].

The consumption of the electrode material C_{el}, kg/m^3, is determined according to Faraday's law:

$$C_{\text{el}} = \frac{ItM_w}{zFV} \tag{17}$$

where M_w is the molecular mass (26.98 g/mol) for Al, z number of electrons transferred (z = 3), F Faraday constant, t the duration of the electrocoagulation process, s.

Table 2

Operating costs of the EC process for all experiments

Experiment	V [dm^3]	U [V]	i [A]	a [€/(kW·h)]	C_{elc} [kWh/m^3]	C_{pump} [kWh/m^3]	b [€/kg]	C_{elt} [kg/m^3]	Operating costs [€/m^3]
1	270	20	5	0.13	0.56	0.72	1.54	0.019	0.19
2	270		3		0.33	0.72		0.011	0.15
3	810		5		0.19	0.54		0.006	0.10
4	810		3		0.11	0.54		0.004	0.09
5	270		5		0.56	0.72		0.019	0.19

Due to the process parameters values used in the experiments, as well as the electricity consumption, electricity consumption by the pump, number of the electrodes in the reactor (two electrodes), operational tank volume, the mass of the electrodes used to generate metal ions and the cost of the electrode material, operational costs are given in Table 2.

According to the operational parameters of the most efficient experiment (experiment 3, Q = 0.15 dm^3/s, U = 20 V, I = 5 A, t_{EC} = 5400 s, V_1 = 0.09 m^3), the electricity consumption of the EC process is C_{el} = 0.19 kWh/m^3 and the electricity consumption of the pump is C_{pump} = 0.54 kWh/m^3. The electrode material consumption is $C_{electrode}$ = 0.006 kg/m^3. Given the calculated unit values, the total operational cost of the Experiment 3 is 0.10 EUR/m^3. Slightly lower costs were realized in Experiment 4 due to the lower current, which also caused significantly lower removal efficiency. Also, total operational cost of the Experiment 3 can be expressed per removed PO_4^{3-}-P . In that case the cost is 3.6 €/kg PO_4^{3-}-P . This cost is difficult to compare with conventional methods such as biological or chemical removal of phosphorus due to different water treatment plants configurations and procedures, or different costing methodologies (some include sludge handling costs or chemicals transport cost others don't), but these costs are reported to be in between 0.9 and 440 €/kg[1] of removed P [27], [28], [29], and what makes EC the competitive technology.

6. CONCLUSION

EC process for the removal of phosphate (PO_4^{3-}-P) was analyzed using a batch full--scale reactor with aluminum electrodes to obtain measured values, according to which the parameterization of the numerical model was performed. Mostly, a linear change of EC process parameters was observed during the tests, which is consistent with similar studies.

The efficiency of the EC process, observed through the reduction of the PO_4^{3-}-P concentration, is primarily dependent on applied current density for the same volume of treated water. After 90 min of EC process, by using the initial NaCl concentration of 2 g/dm^3, current density of 75 A/m^2 on the Al electrodes, and the flow rate Q of 0.15 dm^3/s through the reactor, the PO_4^{3-}-P concentration was reduced by 90%. In the experiment with three times less flow rate and the same values of the rest operating parameters, the PO_4^{3-}-P concentration was reduced by 88%, indicating that the flow rate through the reactor is a less influential parameter. This is also evident from the comparison of experiments 2 and 4 where the current density was 45 A/m^2.

However, a higher flow rate has a better influence on operating costs since more water is treated in the same period. This also indicates that the possibility of achieving

a continuous EC process, in which, ultimately, water flow between electrodes in only one cycle, needs to be further investigated. The estimated operating costs show that the process parameters should be carefully investigated before obtaining their optimal values for a specific case. A comparison of experiments 1 and 5 or 3 and 4 shows that operating costs can be similar for different contamination removal efficiencies.

The concept of the presented numerical model is an innovative methodological approach to modeling the EC process. It includes the basic physical processes related to the phosphate removal mechanism for which the corresponding equations are given. The model shows satisfying results regarding the PO_4^{3-}-P concentration change and distribution. Also, the average measured and modeled flow velocities show satisfying match. This leads to the conclusion that the parameterization of the hydrodynamic part of the numerical model is also properly implemented. Since the present form of the model contains a hydraulic component, it can be used to investigate the influence of the reactor design elements on the effectiveness of the EC process, as well as to investigate the possibility of designing a continuous EC reactor/device.

ACKNOWLEDGMENTS

This work was supported in part by the Croatian Science Foundation under the project PRIMEUS (UIP2020-02-1160).

REFERENCES

[1] SINCERO G.A., *Physical-chemical Treatment of Water and Wastewater*, CRC Press, Boca Raton, Florida, 2003.

[2] European Commission, *Council directive 91/271/EEC of 21 May 1991 concerning urban waste-water treatment*, Off. J. Eur. Union, L135, 1991, 40–52.

[3] TCHOBANOGLOUS G., BURTON F.L., *Wastewater engineering: treatment, disposal, reuse*, McGraw-Hill, 1991.

[4] GRUBB D.G., GUIMARAES M.S., VALENCIA R., *Phosphate immobilization using an acidic type F fly ash*, J. Hazard. Mater., 2000, 76, 217–236. DOI: 10.1016/S0304-3894(00)00200-4.

[5] YILDIZ E., *Phosphate removal from water by fly ash using crossflow microfiltration*, Sep. Purif. Technol., 2004, 35, 241–252. DOI: 10.1016/S1383-5866(03)00145-X.

[6] IRDEMEZ S., YILDIZ Y.S., TOSUNOGLU V., *Optimization of phosphate removal from wastewater by electrocoagulation with aluminum plate electrodes*, Sep. Purif. Technol., 2006, 52, 394–401. DOI: 10.1016/j.seppur.2006.05.020.

[7] HAKIZIMANA J.N., GOURICH B., CHAFI M., STIRIBA Y., VIAL C., DROGUI P., NAJA J., *Electrocoagulation process in water treatment: A review of electrocoagulation modeling approaches*, Desal., 2017, 404, 1–21. DOI: 10.1016/j.desal.2016.10.011.

[8] MOLLAH M.Y.A., SCHENNACH R., PARGA J.R., COCKE D.L., *Electrocoagulation (EC) – science and application*, J. Hazard. Mater. B, 2001, 84, 29–41. DOI: 10.1016/S0304-3894(01)00176-5.

[9] IRDEMEZ S., DEMIRCIOGLU N., YILDIZ Y.S., BINGUL Z., *The effects of current density and phosphate concentration on phosphate removal from wastewater by electrocoagulation using aluminum and iron plate electrodes*, Sep. Purif. Technol., 2006, 52, 218–223. DOI: 10.1016/j.seppur.2006.04.008.

[10] CHEN X., CHEN G.C., YUE P.L., *Separation of pollutants from restaurant wastewater by electrocoagulation*, Sep. Purif. Technol., 2000, 19, 65–76. DOI: 10.1016/S1383-5866(99)00072-6.
[11] ECKENFELDER Jr. W.W., *Industrial Water Pollution Control*, 2nd Ed., McGraw-Hill, 1989.
[12] KABDASLI I., ARSLAN-ALATON I., OLMEZ-HANCI T., TUNAY O., *Electrocoagulation applications for industrial wastewaters. A critical review*, Environ. Technol. Rev., 2012, 1 (1), 2–45. DOI: 10.1080/21622515.2012.715390.
[13] KOBYA M., CAN O.T., BAYRAMOGLU M., *Treatment of textile wastewater by electrocoagulation using iron and aluminum electrodes*, J. Hazard. Mater., 2003, 16–178. DOI: 10.1016/S0304-3894(03)00102-X.
[14] PIZZI N.G., *Water Treatment Operator Handbook*, American Water Works Association, 2011.
[15] WEBER W.J., *Physicochemical Processes for Water Quality Control*, John Wiley, 1972.
[16] FERZIGER J.H., *Simulation of incompressible turbulent flows*, J. Comp. Phys., 1987, 69 (1), 1–48. DOI: 10.1016/0021-9991(87)90154-9.
[17] RASMUSSEN E.B., *Three-dimensional hydrodynamic models*, [In:] M.B. Abbott, N.A. Price, (Eds.), *Coastal, Estuarial and Harbour Engineer's Reference Book*, Chapman and Hall, London 1993, 109–116.
[18] CASULLI V., *A semi-implicit finite difference method for non-hydrostatic, free-surface flows*, Int. J. Num. Meth. Fluids, 1999, 30, 425–440. DOI: 10.1002/(SICI)1097-0363(19990630)30:4<425::AID-FLD847>3.0.CO;2-D.
[19] ABBOTT M.B., BASCO D.R., *Computational Fluid Dynamics, an Introduction for Engineers*, Longman Scientific and Technical, 1989.
[20] RICHTMEYER R.D., MORTON K.W., *Difference Methods for Initial-Value Problems*, Krieger Publishing Company, 1994.
[21] VESTED H.J., JUSTESEN P., EKEBJÆRG L., *Advection-dispersion modelling in three dimensions*, Appl. Math. Modell., 1992, 16 (10), 506–519. DOI: 10.1016/0307-904X(92)90001-J.
[22] GROSS E.S., BONAVENTURA L., ROSATTI G., *Consistency with continuity in conservative advective schemes for free surface models*, Int. J. Numer. Meth. Fluids, 2002, 38, 307–327. DOI: 10.1002/fld.222.
[23] RODI W., *Turbulence Models and Their Application in Hydraulics. A State of the Art Review*, IAHR Monographs, CRC Press, 1993.
[24] SMAGORINSKY J., *Some historical remarks on the use of nonlinear viscosities*, [In:] B. Galperin, S. Orszag (Eds.), *Large Eddy Simulations of Complex Engineering and Geophysical Flows*, Cambridge University Press, 1993, 3–36.
[25] LAI C.L., LIN S.H., *Treatment of chemical mechanical polishing wastewater by electrocoagulation: system performances and sludge settling characteristics*, Chemosphere, 2004, 54, 235–24.2. DOI: 10.1016/j. chemosphere.2003.08.014.
[26] Pedrollo, *General Catalogue 2005*, 16–19. Accessed: September 20, 2019, http://www.tekhar.com/Programma/Pedrollo/C2002UK.pdf
[27] GOEHRING L.D., STEENHUIS T.S., BROOKS A., ROSENWALD M.N., CHEN J., PUTNAM V.J., *Cost-Effective Phosphorus Removal from Secondary through Mineral Adsorption*, Technical Report No. 36, Cornell University, Essex County Planning Department for Lake Champlain Basin Program, 1999.
[28] BASHAR R., GUNGOR K., KARTHIKEYAN K.G., BARAK P., *Cost effectiveness of phosphorus removal processes in municipal wastewater treatment*, Chemosphere, 2018, 197, 280–290. DOI: 10.1016/j.chemosphere.2017.12.169.
[29] DUNNE E.J., COVENEY M., HOGE V., CONROW R., NALEWAY R., LOWE E., BATTOE L., WANG Y., *Phosphorus removal performance of a large-scale constructed treatment wetland receiving eutrophic lake water*, Ecol. Eng., 2015, 79. DOI: 10.1016/j.ecoleng.2015.02.003.